INVESTIGATING THE POTENTIAL OF ZIGZAG SCHEME MONITORING USING THE FLUVIAL ACOUSTIC TOMOGRAPHY SYSTEM

MB AlSawaf Kitami Institute of Technology, Kitami, Hokkaidō, Japan
Y Watanabe Kitami Institute of Technology, Kitami, Hokkaidō, Japan
A Sasaki Hokkaisuikō consultant corporation, Kitami, Hokkaidō, Japan
K Inoue Hokkaisuikō consultant corporation, Obihiro, Hokkaidō, Japan

1 INTRODUCTION

Within the past few decades, underwater acoustic tomography-based applications have received an increasing interest in river engineering, offering promising solutions for accurate and continuous river flow monitoring [1]. The feasibility of using underwater acoustic tomography for streamflow measurement had been documented by several works by investigating its accuracy, limitations, and potential benefits [2–5]. For example, works of [6,7], utilized the fluvial acoustic tomography (FAT) system in measuring river flow. In the case of the FAT system, river flow is basically determined based on the travel-time approach. However, one of the main challenges in measuring river flow by means of the travel-time approach is the necessity of accurate determination of the flow direction.

Determining flow direction is one of the most exciting and challenging applications of travel-time principles. Pioneering studies by [8,9], explored its estimation using these principles, primarily focusing on a “cross-path configuration”. On the other hand, Bahreinimotlagh et al., [9] sought out to estimate flow direction within a unidirectional stream, while Al Sawaf et al., [7] investigated deeply, discussed the inflow direction computation in a dam lake. Their approach cleverly divided the “cross-path” formed by two acoustic lines into four quadrants, analyzing the time differences between each transducer pair and introduced comprehensive guidelines of flow direction and river discharge using cross-path configuration. Additionally, Sloat and Gain [8], proposed another intriguing method utilizing “multi-sectional paths” where this configuration involves more than four acoustic stations to estimate flow direction via the travel-time approach. Recently, Al Sawaf et al., [1] introduced the guidelines of flow direction and river discharge computation using a “triangular configuration” of three tomographic systems placed in unidirectional rivers. However, precise monitoring of smaller and shallower streams holds value not only for discharge measurements but also for understanding into the complex of river channel and river bank scouring and erosion processes under shallow flow conditions.

Therefore, the aim of this study is to shed light on continuous monitoring of streamflow using an innovative tomographic system. The novelty of this work is to propose and discuss the primary guidelines on flow direction estimation in rivers using a zigzag distribution of underwater acoustic tomography systems.

2 MATERIALS AND METHODS

2.1 Study Site and Tomographic Measurement

Field measurements were carried out in the Tokoro River which is the largest river in the Okhotsk Region of Japan located in Kitami city of Hokkaidō Island. The river channel has a 120 km length, with an average width of 40 m near the observation site, and a basin area of 1930 km^2.

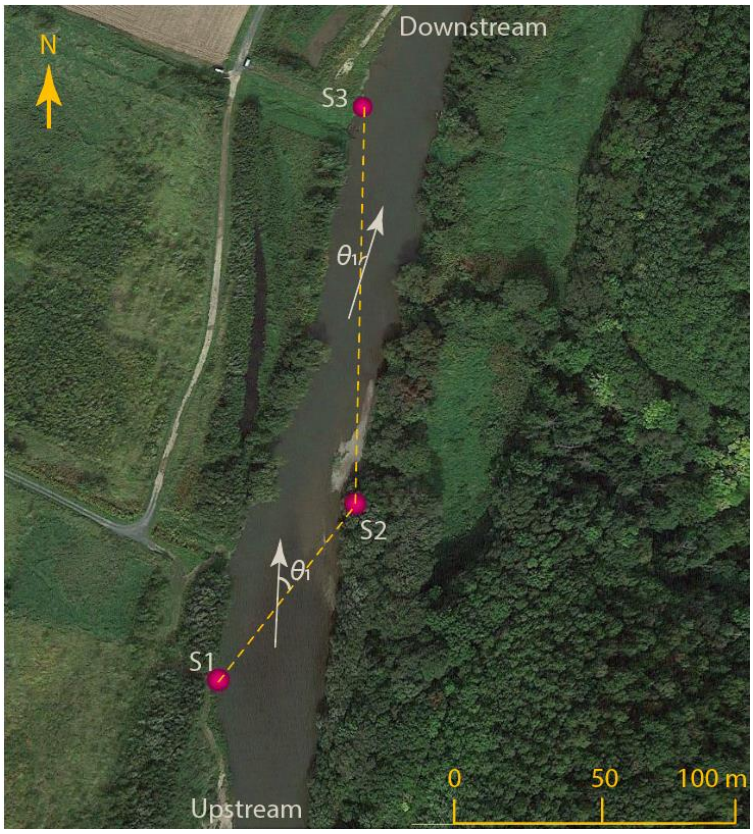

Figure 1: Representation of the monitoring site and the placement of the tomographic stations

In this work, acoustic measurements of river flow were conducted using the fluvial acoustic tomography (FAT) system. Figure 1 illustrates the tomographic measurement style that was conducted using the FAT system. In this observation, three FAT systems were arranged in a zigzag pattern across the river site. As can be seen in Fig. 1, one system (i.e., S2) was positioned on the right bank, while the other two systems (i.e., S1 and S3) were placed on the left bank. The backbone of acoustic measurement by means of the FAT system is the travel-time approach. In other words, the FAT system measures the river flow by measuring the travel-time of sound waves between each pair of underwater transducers, such as S1 and S2 as depicted in Fig. 1. This allows to estimate the stream velocity along the transmission path (u_1) using the following equation:

$$u_1 = \frac{L_1}{2} \times \left(\frac{1}{t_{s1}} - \frac{1}{t_{s2}}\right) \tag{1}$$

where L_1 is the direct distance between transducers S1 and S2, the travel-times t_{S1} and t_{S2} represent the time it takes for an acoustic signal to travel from S1 to S2 and vice versa, respectively. As a result, the cross-sectional stream velocity (v_1) and flow (Q_{FAT}) using FAT can be computed as:

$$v_1 = \frac{u_1}{\cos\theta_1} \tag{2}$$

$$Q_{FAT} = u_1 \times A_1 \times \tan\alpha_1 \tag{3}$$

where A_1 denotes the cross-sectional area along the S1S2, $\alpha_1$is the flow direction angle between the transmission cross-section S1S2 and the flow direction. The FAT system uses underwater transducers that emit sound waves in all directions (i.e., omnidirectional) at a frequency of 58 (kHz).

These sound signals were triggered together concurrently, every 30 seconds. To make sure that all the transducers trigger their sound waves at the exact same moment, the FAT system was supplied with GPS receivers capable to provide a precise signal every second and a reference frequency of 10 (MHz).
To measure the temporal variations in the cross-sectional area, water level, HOBO®_U20 pressure loggers were clipped onto the transducers at S1, S2, and S3. These loggers recorded the water levels in the site every 5 minutes. Therefore, the cross-sectional area along S1S2 and S2S3 were continuously calculated by integrating the riverbed along S1S2 and S2S3 with the water level records.

2.2 Flow Direction Computation Based on Zigzag Tomographic Scheme

The novelty in this research is in trying to propose the first set of guidelines for estimating river flow direction using a zigzag tomographic scheme. Figures (2&3) depict the flowchart and simplify this estimation process. First of all, it is crucial to mention that this method relies on the assumption that the flow rate across both cross-sections (S1-S2 and S2-S3) is equal or nearly identical. Hence, this assumption allows us to apply the principle of flow continuity, where the flow entering one section (i.e., S1-S2) must equal the flow exiting the next cross-section (i.e., S2-S3). As a result, the flow rates through S1S2 (Q_{S1S2}) and S2-S3 (Q_{S2S3}) are essentially the same. Therefore, one can write:

$$Q_{S1S2} = Q_{S2S3} \tag{4}$$

Equation (4) can be expressed as:

$$u_1 \times A_1 \times \tan\alpha_1 = u_1 \times A_2 \times \tan\alpha_2 \tag{5}$$

where u_2, A_2 are the cross-sectional mean velocity, and area along S2-S3, respectively, and α_2 is the angle between the acoustic path S2-S3 and streamflow direction.

To start with, the first step as can be seen in Fig. 2 is to determine the flow direction domain. In the case of the current monitoring site, the flow is unidirectional, that is to say, the flow is expected to be from the upstream direction to the downstream, and hence both stream velocity components along S1-S2 (i.e., u_1) and S2-S3 (i.e., u_2) are positive, thus, the flow domain should be in the intersection zone of both transmission line axes. More specifically, in the intersection of the first and second quadrants (Q1, Q2) of ((X, Y) & (V, W)) as illustrated in Fig. 3 (a, b), because river flow through (Q3, Q4) is negative. Hence, the flow domain in this case equals to 180°-2φ, and four cases can be distinguished as presented in Fig. 3.
At each time step (t_i), the instantaneous flow angles (α_1& α_2) can be estimated by examining the status of the velocity vectors (u_1 & u_2) and cross-sectional areas (A_1 & A_2). As illustrated in Fig. 2 and Fig. 3c, if the flow direction in the region of case 1, the flow direction over S1-S2 and S2-S3 can be expressed as: $\alpha_2 = \varphi + \alpha_1$. By substituting in Eq. (5), flow angle (α_1) can be expressed as:

$$\alpha_1 = \tan^{-1}\left(\frac{u_2 \times A_2}{u_1 \times A_1} \times \tan(\varphi + \alpha_1)\right) \tag{6}$$

Equation (6) can be expressed as:

$$\alpha_1 = \cos^{-1}\left(\frac{1}{2}\sqrt{-\frac{(-3+\cos(2\phi))A_1u_1 + 2\cos(\phi)(\cos(\phi)A_2u_2 + \sqrt{\cos(\phi)^2A_1^2u_1^2 + (-3+\cos(2\phi))A_1A_2u_1u_2 + \cos(\phi)^2A_2^2u_2^2})}{A_1u_1 - A_2u_2}}\right. \tag{7}$$

As can be seen in Fig. 2, if the flow direction does not meet the condition of case 1, then the next step is to consider if the condition of case 2 is valid, thus, the flow direction can be expressed as:

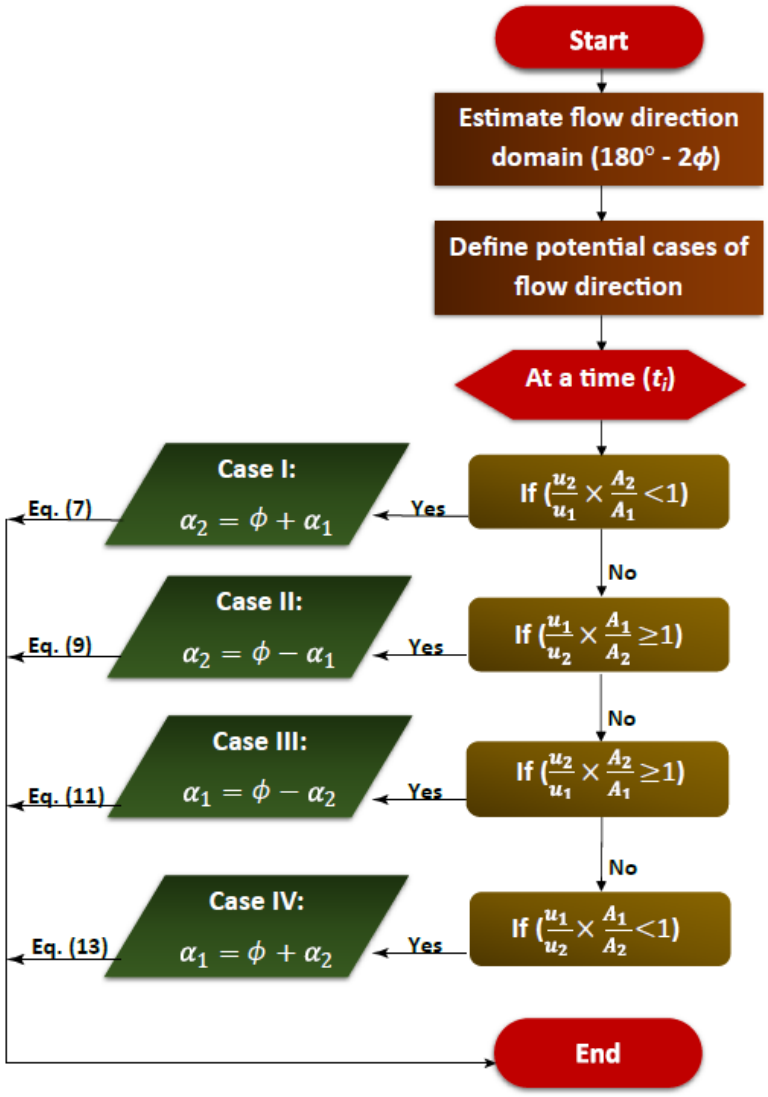

Figure 2: Flowchart of flow direction estimation using a zigzag tomographic scheme

$$\alpha_1 = \tan^{-1}\left(\frac{u_1 \times A_1}{u_2 \times A_2} \times \tan(\phi - \alpha_1)\right) \tag{8}$$

Equation (8) can be written as:

$$\alpha_1 = \cos^{-1}\left(\frac{1}{2}\sqrt{\frac{-(-3+\cos(2\phi))A_1u_1 + 2\cos(\phi)(\cos(\phi)A_2u_2 + \sqrt{\cos(\phi)^2A_1^2u_1^2 - (-3+\cos(2\phi))A_1A_2u_1u_2 + \cos(\phi)^2A_2^2u_2^2)}}{A_1u_1 + A_2u_2}}\right. \tag{9}$$

Again, if the flow direction does not meet the condition of case 2, then the next step is to verify the condition of case 3 is valid, hence, the flow direction can be expressed as:

$$\alpha_2 = \tan^{-1}\left(\frac{u_1 \times A_1}{u_2 \times A_2} \times \tan(\phi - \alpha_1)\right) \tag{10}$$

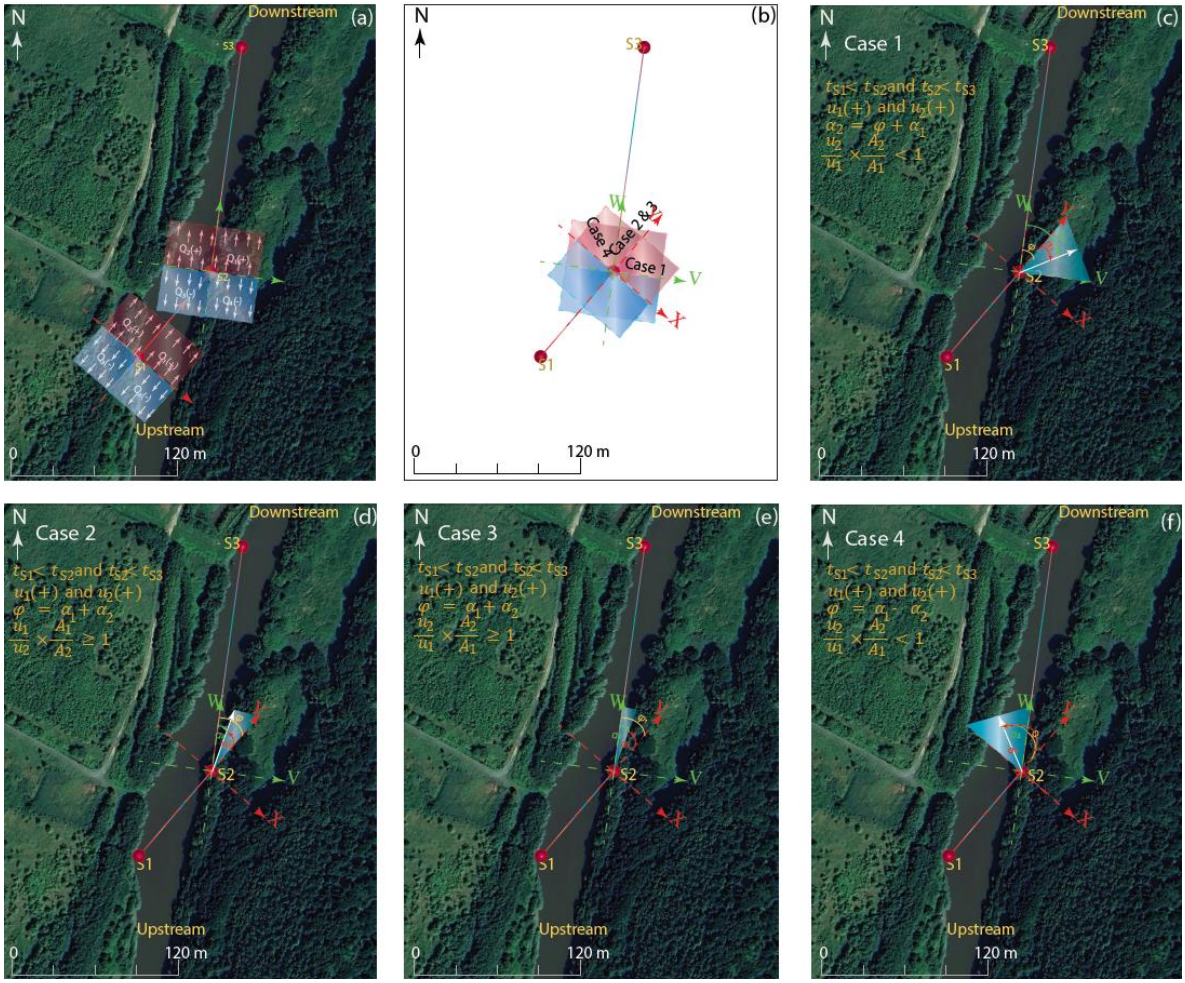

Figure 3: Flow direction cases; a, b) basic domain illustration; c) case 1; d) case 2; e) case3; and f) case 4

In the same manner, Eq. (10) can be written as:

$$\alpha_2 = \cos^{-1}\left(\frac{1}{2}\sqrt{\frac{2\cos(\phi)^2 A_1 u_1 + 3A_2 u_2 - \cos(2\phi)A_2 u_2 + 2\cos(\phi)\sqrt{\cos(\phi)^2 A_1^2 u_1^2 - (-3+\cos(2\phi))A_1 A_2 u_1 u_2 + \cos(\phi)^2 A_2^2 u_2^2}}{A_1 u_1 + A_2 u_2}}\right) \quad (11)$$

Finally, if the flow direction does not verify the condition of case 3, then the last expected step is to have the flow direction in the last case, i.e., case 4, thus, the flow direction can be expressed as:

$$\alpha_2 = \tan^{-1}\left(\frac{u_1 \times A_1}{u_2 \times A_2} \times \tan(\phi + \alpha_1)\right) \quad (12)$$

As a result, Eq. (12) can be written as:

$$\alpha_2 = \cos^{-1}\left(\frac{1}{2}\sqrt{\frac{2\cos(\phi)^2 A_1 u_1 - 3A_2 u_2 + \cos(2\phi)A_2 u_2 - 2\cos(\phi)\sqrt{\cos(\phi)^2 A_1^2 u_1^2 + (-3+\cos(2\phi))A_1 A_2 u_1 u_2 + \cos(\phi)^2 A_2^2 u_2^2}}{A_1 u_1 - A_2 u_2}}\right) \quad (13)$$

3 RESULTS AND DISCUSSION

Figures (4a & 5a) compares the recorded travel-times recorded at the upstream and downstream stations. In particular, Fig. 4a shows the temporal variations in travel-times recorded along S1-S2 from the upstream to the downstream station (i.e., t_{s1}, red), as well as the travel-times recorded from the downstream to the upstream stations (i.e., t_{s2}, blue). In the same manner, Fig. 5a compares the temporal variations in travel times recorded along S2-S3 from the upstream to the downstream station (i.e., t_{s2}, red), as well as the travel-times recorded from the downstream to the upstream stations (i.e., t_{s3}, blue). In the case of the transmission cross-section along S1-S2, it can be verified that the difference in time (Δt) is positive (Fig. 4b), and therefore the flow velocity along S1-S2 is positive as depicted in Fig. 4c. On the other hand, in the case of the transmission cross-section along S2-S3, it can be noticed that the difference in time was found to be negative (Fig. 5b). In other words, according to Eq. (1) the stream velocity along S2-S3 is negative (Fig. 5c), which is not possible in the case of our observation site. Consequently, the aforementioned assumptions are not valid in this case, and therefore, additional investigations are necessary to deeper understanding. Nonetheless, it can be said that according to our current assessment it can be justified due to the presence of local, secondary flow contribution that affected the performance of sound speed near S3 station.

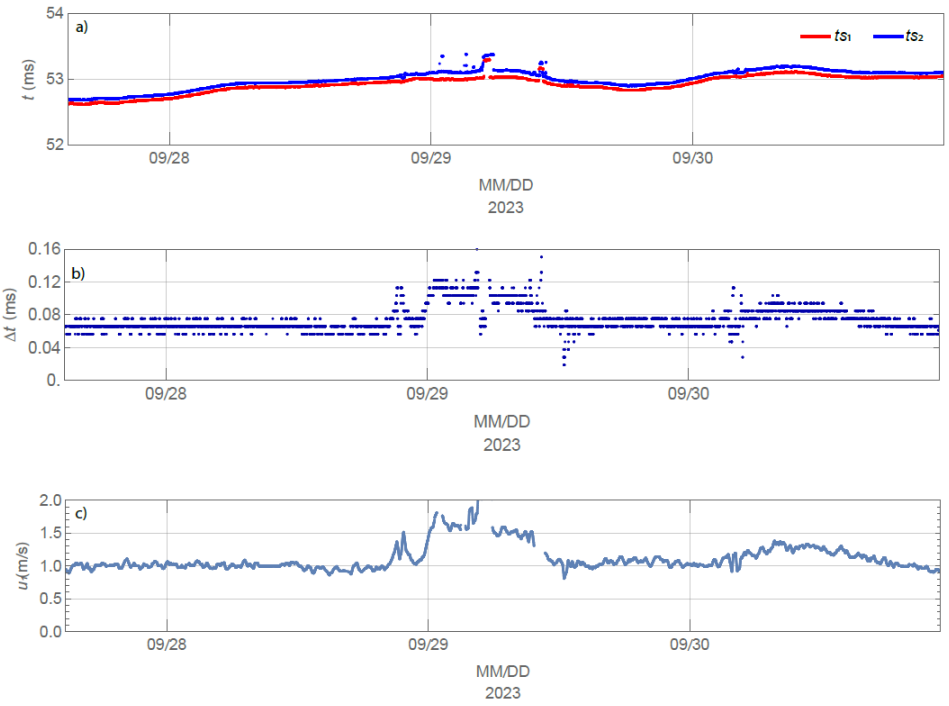

Figure 4: Time-series of a) temporal variations in travel-times from upstream to downstream (red), and from downstream to upstream (blue); b) difference in travel-times; c) cross-sectional average velocity along S1-S2

Fortunately, streamflow direction was estimated by regression analysis using another reference record. In simple words, the flow direction term (α_1) can be computed using the river discharge estimated by the Rating Curves approach (Q_{RC}) using Eq. (3). Accordingly, river flow dynamics during three different cases (normal flow conditions and flood) were investigated and presented in Fig. 6. As can be seen in Fig. (6a & 6e), the water level raised up to 4.5 and 5.5 m, respectively, i.e., flood conditions. Alternatively, the water level during the recorded event in Fig.(6i) represents the flow during normal flow condition. In addition, Fig. 6(b, f, i), exhibits the temporal variations in the river discharge (Q_{FAT}) as obtained by the FAT system. To verify the accuracy of our tomographic measurements, we compared the river flow estimated by the FAT system with other discharge records obtained by other instruments deployed in the same location, i.e., H-ADCP, STIV, and the rating curve results. Interestingly, it can be seen that the flow estimated by the FAT system was in a very good agreement with the flow obtained by other approaches (Fig.6). Unfortunately, the missing period

shown in the figures, indicate that these data were not accepted due to the fact that their trave-times were not reliable Fig. 6 (d, h).

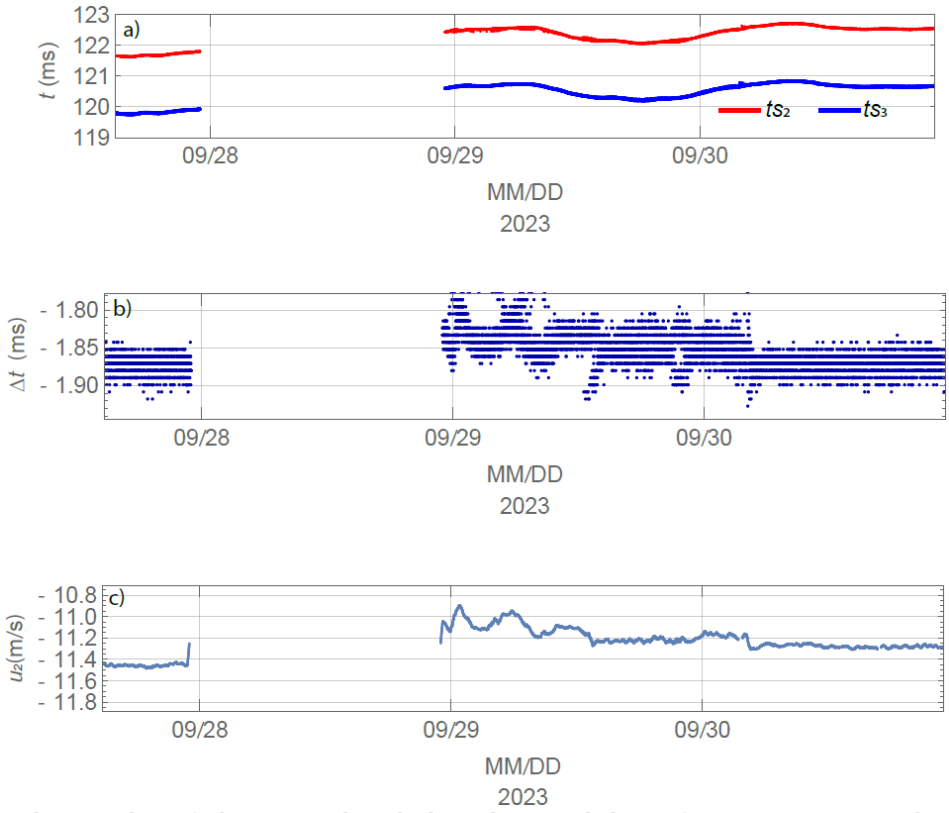

Figure 5: Time-series of a) temporal variations in travel-times from upstream to downstream (red), and from downstream to upstream (blue); b) difference in travel-times; c) cross-sectional average velocity along S2-S3

Alternatively, to have a better understanding regarding the potential errors, the uncertainty percentage was estimated. Encouragingly, it can be seen, the uncertainty level was ranged between -10 to 10%, approximately, with minor period up to 25% as depicted in Fig. 6 (c, g, k).

4 CONCLUSIONS

In this work, we aimed to present and share a case of our monitoring program to measure river flow using an advanced tomographic system. In particular, we aimed to use the FAT system to continuously measure the flow direction and river discharge in a unidirectional stream. In addition, we tried to propose the first guidelines for continuous river flow direction and streamflow in a zigzag plane. In fact, the proposed guidelines appear to be interesting and promising. Unfortunately, we could not get demonstration using field data owing to site-based challenges. On the other hand, river flow estimated by the FAT system seemed to be reliable in comparison to other independent records. Future investigations are necessary to improve the current method and have fruitful applications.

ACKNOWLEDGMENT

This work was funded by the river centre of Hokkaidō and Charitable Trust Ono Acoustics Research Grant Fund. In addition, this work would not be possible without the support of Hokkaisuikō Consultant Co., Ltd.

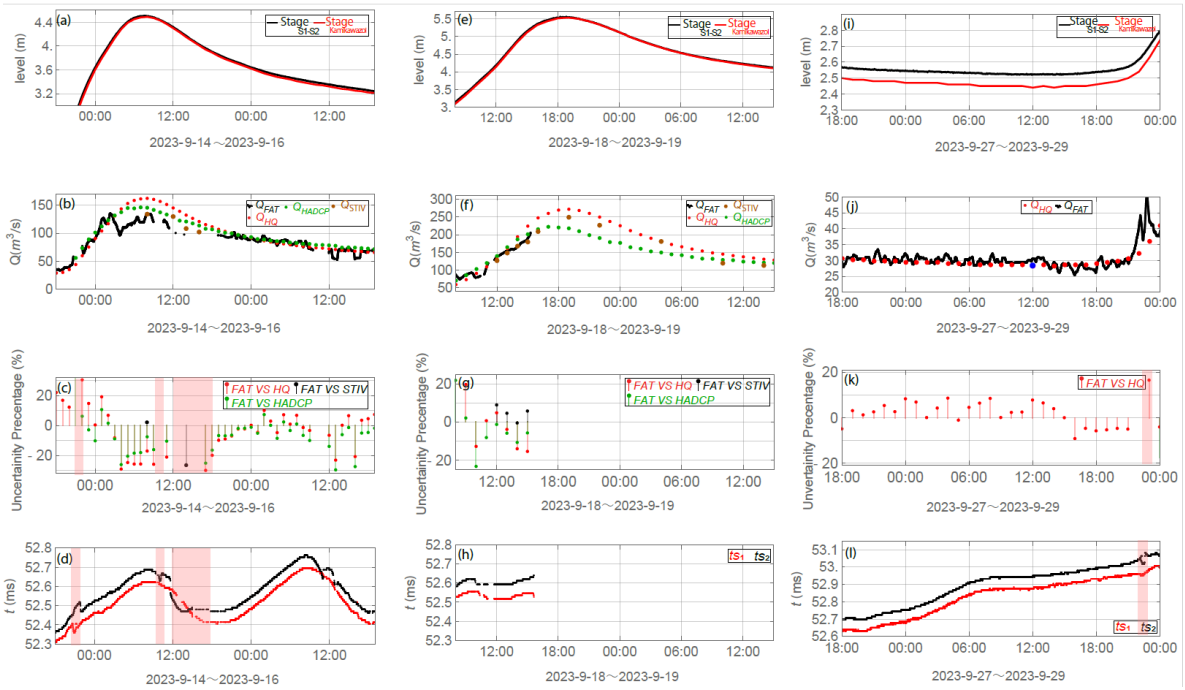

Figure 6: Time-series of a), b), c), river stage; b), f), j), river discharge; c), g), k), uncertainty percentage; d), h), l), temporal variations in travel-times

REFERENCES

1. Al Sawaf MB, Kawanisi K, Gusti GNN, Khadami F, Xiao C, Bahreinimotlagh M. Continuous measurement of flow direction and streamflow based on travel time principles using a triangular distribution of acoustic tomography systems. J Hydrol. 2023;617:128917. doi: 10.1016/j.jhydrol.2022.128917.
2. Xiao C, Kawanisi K, Al Sawaf MB, Zhu XH. Assessment of flood dynamics in a mountain stream using high-resolution river flow records. Hydrol Process. 2023;37(3). doi: 10.1002/hyp.14841.
3. Al Sawaf MB, Kawanisi K, Xiao C. Measuring Low Flowrates of a Shallow Mountainous River Within Restricted Site Conditions and the Characteristics of Acoustic Arrival Times Within Low Flows. Water Resour Manag. 2020;34(10):3059–3078. doi: 10.1007/s11269-020-02557-w.
4. Xiao C, Kawanisi K, Torigoe R, Al Sawaf MB. Mapping tidal current and salinity at a shallow tidal channel junction using the fluvial acoustic tomography system. Estuar Coast Shelf Sci. 2021;258:107440. doi: 10.1016/j.ecss.2021.107440.
5. Danial MM, Kawanisi K, Al Sawaf MB. Characteristics of tidal discharge and phase difference at a tidal channel junction investigated using the fluvial acoustic tomography system. Water (Switzerland). 2019;11(4):857. doi: 10.3390/w11040857.
6. Nguyen HT, Kawanisi K, Al Sawaf MB. Acoustic Monitoring of Tidal Flow and Salinity in a Tidal Channel. J Mar Sci Eng. 2021;9(11):1180. doi: 10.3390/jmse9111180.
7. Al Sawaf MB, Kawanisi K, Xiao C, Gusti GNN, Khadami F. Monitoring Inflow Dynamics in a Multipurpose Dam Based on Travel-time Principle. Water Resour Manag. 2022;36(8):2589–2610. doi: 10.1007/s11269-022-03161-w.
8. Sloat J V, Gain WS. Application of acoustic velocity meters for gaging discharge of three low-velocity tidal streams in the St. Johns River Basin, northeast Florida. 1995;iv, 26 p.
9. Bahreinimotlagh M, Kawanisi K, Danial MM, Al Sawaf MB, Kagami J. Application of shallow-water acoustic tomography to measure flow direction and river discharge. Flow Meas Instrum. 2016;51:30–39. doi: 10.1016/j.flowmeasinst.2016.08.010.